Optics Communications 284 (2011) 2345–2350

Contents lists available at ScienceDirect

Optics Communications

journal homepage: www.elsevier.com/locate/optcom

Static and dynamic analysis of an all-optical inverter based on a Vertical Cavity Semiconductor Optical Amplifier (VCSOA)

Veronica Gauss [a,*], Antonio Hurtado [b], Doug Jorgesen [a], Michael J. Adams [b], Sadik Esener [a]

[a] Department of Electrical and Computer Engineering, University of California, San Diego, 9500 Gilman Dr., La Jolla, CA 92093, USA
[b] School of Computer Science and Electronic Engineering,University of Essex, Wivenhoe Park, CO4 3SQ Colchester, UK

ARTICLE INFO

Article history:
Received 3 August 2010
Received in revised form 7 December 2010
Accepted 10 January 2011
Available online 26 January 2011

Keywords:
Nonlinear optics
Optical bistability
All-optical signal processing
All-optical logic gate
All-optical inverter
Vertical cavity semiconductor optical amplifier

ABSTRACT

We report the static and dynamic properties of an all-optical inverter based on an 850 nm Vertical Cavity Semiconductor Optical Amplifier (VCSOA). The inverter exhibits low switching power requirements (~15 μW), large on/off contrast ratio (>11 dB), and high speed operation (~1.4 GHz). Large and small signal measurements show that the speed of operation and the on/off contrast ratio improve with increased bias current. This holds important prospects for the development of VCSOA-inverters for high-speed, low-power optical logic applications. Finally, a theoretical model of the VCSOA-inverter has been employed giving good agreement with experiments.

1. Introduction

All-optical logic based on Vertical Cavity Surface-Emitting Lasers and Semiconductor Amplifiers (VCSELs and VCSOAs) has been the subject of extensive research in recent years because of the potential applications in all-optical signal processing [1–12]. In particular, all-optical VCSOA inverters operating at 850 nm wavelength may play an important role in future short-reach and local area networks since 850 nm technology continues to dominate this market [13,14]. Their low manufacturing costs, small size, low electrical and optical power consumption, and ease of integration make them ideal for short distance high density applications. In addition, as with their electrical counterparts, VCSOA inverters are cascadable and can be combined in various configurations to provide a myriad of logic operations [5–7,12].

VCSOA inverters operate on the principles of optical nonlinearity, cross-gain modulation (XGM), and polarization gain anisotropy [5]. Of key interest, however, is the performance of these inverters since they are intended for high-speed all-optical logic applications. One such application may be in high-speed 850 nm ethernet short-reach and local area networks since VCSOA inverters are based on VCSEL technology which is already prevalent in these networks. In addition, demand for higher data rates in these networks is driving the development of higher performance 850 nm-VCSELs. These new VCSELs increase bandwidth by reducing the effects of electrical transport issues [15–17], and have already demonstrated modulation bandwidths as high as 25 Gbps [15]. Given the similarity of VCSOA and VCSEL structures, advancements in VCSEL design may hold exciting prospects for VCSOA inverters as well.

In the present contribution, we report the large and small signal response of an all-optical inverter based on an 850 nm-VCSOA. As shown in previous experiments [5], inversion in a VCSOA is performed through XGM of two orthogonally-polarized optical injections called the Signal and Optical Bias. We have analyzed experimentally and in simulation the static and dynamic properties of the VCSOA-inverter biased below and above threshold. The static analysis revealed high quality performance characterized by low optical switching power and high on–off contrast ratio. The dynamic analyses showed that the VCSOA-inverter can operate at speeds on the order of 1–2 Gbps. These results, coupled with other important advantages of VCSOAs such as low manufacturing costs, ease of integration in 2D arrays and high coupling efficiency to optical fibers, suggest that these devices may be very promising candidates for all-optical logic applications in short-reach and local area ethernet networks. A theoretical model of the VCSOA-inverter has also been employed in this work and shows good agreement with the experiments.

2. Experimental setup

The setup used for our experiments is illustrated in Fig. 1. A hybrid fiber/free-space design was used in order to interface our free-space VCSOA to the high-speed fiber-coupled modulator and measurement

* Corresponding author. Tel.: +1 619 758 9137.
E-mail address: vgauss@gmail.com (V. Gauss).

0030-4018/$ – see front matter
doi:10.1016/j.optcom.2011.01.010

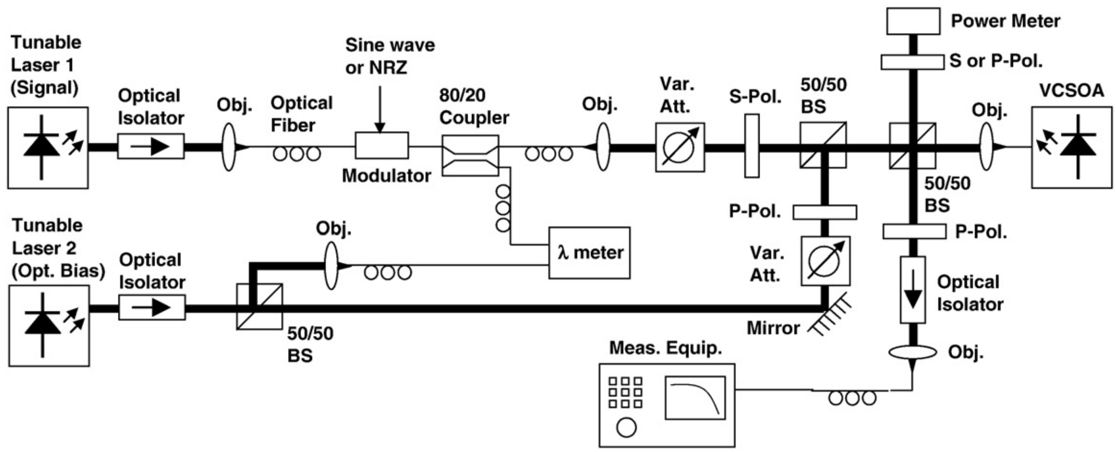

Fig. 1. Experimental setup for comparison of below and above threshold performance of an 850 nm-wavelength VCSOA all-optical inverter.

equipment. The VCSOA was an 850 nm proton-implanted device with a 20 μm aperture and a threshold current of 6.3 mA at a temperature of 23.6 °C. Two tunable lasers were used for the Optical Bias and Signal beams, and optical isolators were positioned at the output of each laser to eliminate back-reflections. The Signal was fiber-coupled into the modulator using a high-quality objective lens, and was modulated with either a sine wave, for small-signal modulation bandwidth measurements, or a non-return-to zero (NRZ) pseudo-random bit stream (PRBS) pattern for large-signal measurements. The Signal was then split using an 80/20 fiber coupler, and the smaller optical power was routed to a wavelength meter. The Optical Bias was also monitored by the wavelength meter via a free-space 50/50 beam-splitter and fiber coupling. The Signal was then coupled back into free-space and routed to the VCSOA. The intensity and polarization of both beams were controlled by variable optical attenuators (VOAs) and individual polarizers in each path as in [5]. The Signal and Optical Bias optical power to the VCSOA were monitored using a power meter, and the output Optical Bias was monitored using a fiber-coupled high-speed photodetector and either an oscilloscope for large signal measurements or a component analyzer for small signal measurements.

3. Theory

The theoretical model used in this work is an extension of the Semiconductor Laser Amplifier (SLA) Analysis reported by Adams et al. [18]. That model has been modified to take into account the structure of a VCSOA. For this purpose we have used the so-called Fabry–Perot approach [19,20]. This approach considers the substitution of the top and bottom Distributed Bragg Reflectors (DBRs) by two highly reflective mirrors which enclose a resonant cavity with an effective length. Under this assumption, we can adapt the rate equation for the carrier concentration given in [18] to the particular structure of the VCSOA. This leads to the following expression:

$$\frac{dN}{dt} = \frac{\eta I}{e\Gamma_1 V} - \left(AN + BN^2 + CN^3\right) - \frac{\Gamma c \xi a(N-n_0)}{n_c}\left[\beta_{eff} S_{1av} + S_{2av}\right]. \quad (1)$$

Where N is the carrier concentration, η is the internal quantum efficiency, I is the bias current applied to the device, e is the electron charge and V is the volume of the cavity. A, B, and C, are the linear, bimolecular and Auger recombination coefficients. Γ is the lateral confinement factor, c is the speed of light in vacuum, ξ is the Gain Enhancement Factor, GEF (as given in [20]), n_c is the refractive index in the cavity, a is the linear material gain coefficient, n_0 is the transparency carrier density and β_{eff} is the spontaneous emission factor. Finally, S_{1av} and S_{2av} express respectively the averaged spontaneous and stimulated photon density.

The inclusion of the spontaneous emission in the modeling is essential to obtain theoretical results when the device is biased above the threshold current. Therefore, the model used in this work is based on the extended formulation of the SLA analysis [18] where the spontaneous emission is taken into consideration. Hence, that model [18] could in principle be used to analyze SLAs operated both below and above threshold. The latter was demonstrated by Pakdeevanich et al. [21] using Adams' model [18] to successfully reproduce experiments on the static properties of Optical Bistability in a Fabry–Perot SLA operated above threshold.

In Eq. (1) Γ_1 refers to the longitudinal confinement factor. This is given by the ratio of the length of the active region, L_a, to the effective cavity length of the VCSOA, L_c, in the form $\Gamma_1 = L_a/L_c$ The use of an effective cavity length arises as a consequence of the Fabry–Perot approach [20]. This effective cavity length accounts for the physical cavity length, L_c (physical separation between both DBRs) as well as the penetration depths for the top (L_t) and bottom mirrors (L_b) [20]. The effective cavity length can be calculated from $L_c = L + L_t + L_b$.

The two orthogonal polarizations of the fundamental transverse mode of the VCSOA have been considered in the theoretical modeling. Hence, the total spontaneous photon density will have two different terms, one for each of the two orthogonal polarizations of the fundamental mode of the device, in the form:

$$S_{1av} = S_{11av} + S_{12av}. \quad (2)$$

The individual terms in (2) can be calculated from the following equations:

$$S_{11av} = \left(\frac{\left(e^{g_1 L_c}-1\right)\left[(1-R_b)\left(1+R_t e^{g_1 L_c}\right) + (1-R_t)\left(1+R_b e^{g_1 L_c}\right)\right]}{g_1 L_c\left(1-R_t R_b e^{2g_1 L_c}\right)} - 2\right)\frac{\Gamma_1 B N^2 n_c}{g_1 c} \quad (3)$$

$$S_{12av} = \left(\frac{\left(e^{g_2 L_c}-1\right)\left[(1-R_b)\left(1+R_t e^{g_2 L_c}\right) + (1-R_t)\left(1+R_b e^{g_2 L_c}\right)\right]}{g_2 L_c\left(1-R_t R_b e^{2g_2 L_c}\right)} - 2\right)\frac{\Gamma_1 B N^2 n_c}{g_2 c}. \quad (4)$$

In Eqs. (3)–(4) R_t and R_b are the top and bottom DBRs reflectivities whereas g_1 and g_2 correspond respectively to the gain per length product for the parallel and the orthogonally-polarized mode of the VCSOA, which are given by the following expressions:

$$g_1 L_c = \Gamma\Gamma_1 \xi a(N-n_0)L_c - \alpha_1 L_c \quad (5)$$

$$g_2 L_c = \Gamma\Gamma_1 \xi a(N-n_0)L_c - \alpha_2 L_c \quad (6)$$